2019A1646 BL14B2

3D Imaging of Liquid Film Migration in Aluminium Alloy after Brazing using Phase-contrast Tomography

Lars-Åke Näslund [a, *], Torkel Stenqvist [a], Daiki Shiozawa [b], Stephen Hall [c], Johan Hektor [c, **], Mårten Edwards [d], Linda Ahl [a], and Robert Moberg [d]

[a] Gränges Sweden AB, [b] Kobe University, [c] Lund University, [d] Uppsala Synchrotronix AB
* Current affiliation: Linköping University, ** Current affiliation: Malmö University

Abstract

An application problem when brazing aluminium is that molten braze alloy may penetrate into the bulk. This may, for example, increase the risk for reduced corrosion resistance and may in the long run lead to coolant leakages in heat exchangers. The phenomenon is poorly understood, which motivates a closer look using synchrotron radiation based 3D imaging. Through phase-contrast tomography at the BL14-B2 beamline at SPring-8 we have recorded 3D images of aluminium sheet materials with different stages of braze alloy penetration where the braze alloy penetration process can be visualized step by step. The characteristic signs of braze alloy penetration has been identified in the 3D images and the project has provided new perspectives on the braze alloy penetration process.

Keywords: Aluminium, Liquid film migration, Controlled atmospheric brazing, Phase-contrast tomography

Background and Purpose

The introduction of braze clad on aluminium (Al) sheets has enabled fast and convenient brazing assembly of complex heat exchangers (HEX) with hard requirements on heat performance, strength, and corrosion resistance [1,2]. The braze clad on aluminium sheets is in most cases an aluminium-silicon (Al-Si) alloy with a solidus of 577 °C. Figure 1(a) shows examples of typical braze clad Al sheet structures in a heat exchanger. A liquid-to-air heat exchanger consists of several parts joined through brazing. The arrows indicate that hot fluid is collected in one tank, pushed through the thin tubes, and cooled as heat is transferred to the fins, which in turn are cooled by the surrounding (forced) air. The cooled fluid is collected in the opposite tank and pushed out in the external circuit that prevents hot parts to become over-heated. Figure 1(b) shows an optical microscopy cross-section image of a joint between a tube and a fin in a heat exchanger. Molten Al-Si braze clad alloy has flown to the narrow space between the tube- and fin materials and formed a joint upon solidification. The microstructure image shows the Al-Si braze clad alloy on the outside and a corrosion inhibiting Al-Zn alloy on the inside (waterside) of the grayer core Al alloy tube material. The core Al alloy appears as grayer, compared with the Al-Si alloy and the Al-Zn alloy because of a homogenous distribution of dispersoids.

During brazing at about 600 °C in a controlled nitrogen gas atmosphere the Al-Si braze alloy in the clad layer liquefies and flows efficiently to the narrow spaces between different heat exchanger parts through the capillary force forming strong joints. However, under certain conditions, e.g., when the material is exposed to cold work prior to the brazing, liquid film migration (LFM) may be a significant problem. LFM is a well-known application problem in the HEX industry and the phenomenon can appear while brazing at about 600 °C. LFM can be described as when the molten braze alloy penetrates into the core material and consequently the filler metal flow to the joints will be reduced, as shown in Figure 2, which causes poor braze joints. A non-linear relationship between the extent of LFM and the applied strain shows that the problem with LFM is high at low material deformation (3-10 %) but reduces with further increases in the applied strain. The decrease in the extent of LFM was shown to be because of core alloy recrystallization during brazing, which reduces the LFM significantly [3]. In addition, LFM will also increase the sensitivity for corrosion of the core aluminium alloy [3]. Figure 3 shows corrosion attacks where LFM has occurred. Hence, under disadvantageous conditions the molten braze alloy may wet grains and penetrate into the aluminium core material causing serious damage to the Al material.

Yoon and Huppman [4] were the first to report LFM during liquid phase sintering of tungsten with nickel. When placed in contact with pure liquid nickel the tungsten grains dissolved at first and then reprecipitated as a solid solution saturated with nickel during the migration of the unreacted liquid into the dissolving grains

of tungsten. The phenomenon of molten braze material penetration into the core alloy has since been observed in many different alloy systems [5]. Behind the front of the liquid film migration, through the core alloy, precipitation will form a dislocation free solid solution consistent with the solidus composition at the brazing temperature [6].

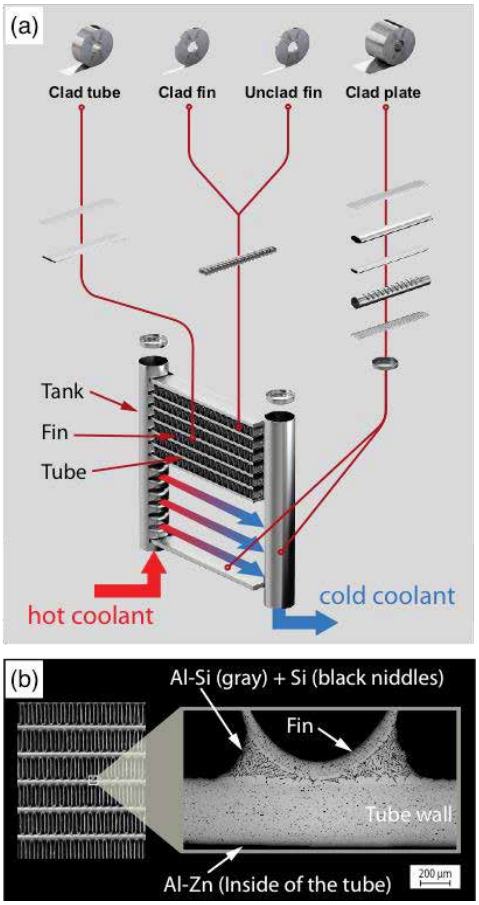

Fig. 1. (a) A liquid-to-air heat exchanger consists of several parts joined through brazing. (b) A cross-section image of a joint between a tube and a fin in a heat exchanger.

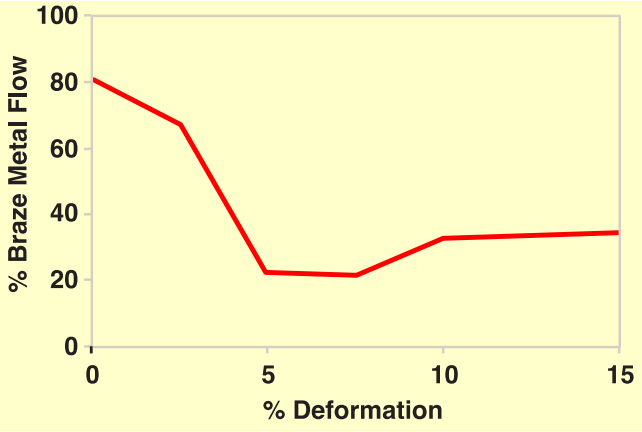

Fig. 2. Small amounts of cold work (3-5%) sharply reduce braze metal flow. More cold work brings some improvement [3].

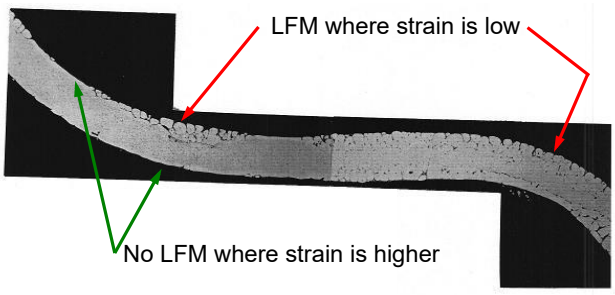

Fig. 3. Cross-section image of a brazed Al sheet that shows liquid film migration (LFM) at areas exposed to low material deformation but no LFM where the strain has been higher. The grain boundaries in the affected areas are prone to corrosion [3].

Recently we presented a three-dimensional X-ray diffraction (3DXRD) study where Al alloy strips, 128 µm thick and 1 mm wide, was investigated [7]. The 3DXRD provided maps of the center-of-mass position of Al grains in the Al alloy samples. In the 3DXRD image of the sample that was braze simulated at one end but not on the other we could distinguish the three zones: the non-"brazed" zone, the fully "brazed" zone, and the transition region between them. Originally for the SPring-8 beamtime at the X-ray absorption beamline BL14-B2 we planned to perform 3DXRD, although with the access to the X-ray scattering beamline SMS P21.2 [8] at the synchrotron radiation facility PETRA III at DESY in Hamburg, Germany, the focus for the BL14-B2 beamtime became phase-contrast X-ray computed tomography (PCX-CT) [9-11] to produce 3D images that show microstructural features in the core Al alloy grains and the distribution of dispersoids in a braze-simulated sample. Since the sample mainly consist of Al and Si, i.e., atoms with low atomic number Z, phase-contrast X-ray imaging shows more sensitivity to density variations in the sample compared to traditional tomography techniques [9-11].

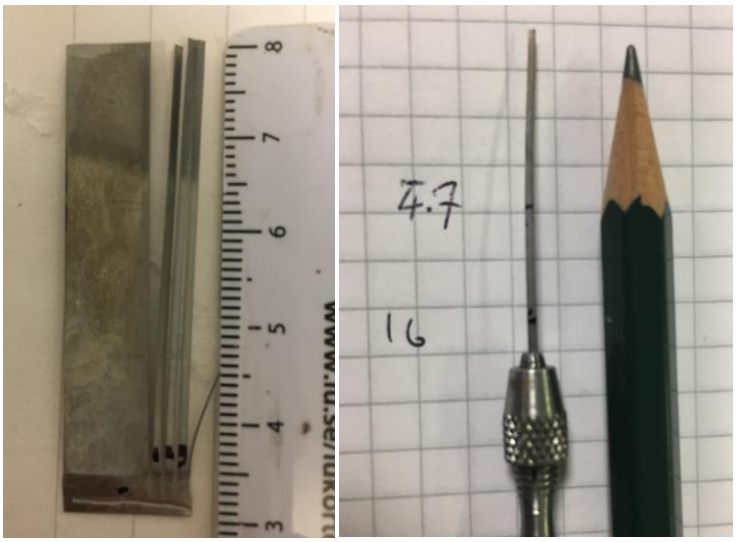

Fig. 4. 1 mm wide and 40 mm long strips along the transition region from the non-"brazed" zone to the "brazed" zone.

Experimental Summary

The 128 µm thick core material selected for this study was an Al alloy with 1.6 % manganese (Mn), 1.5 % zinc (Zn), 0.8 % silicon (Si), 0.25 % iron (Fe), and < 0.1 % zirconium. On one side of the rolled Al sheet there was an 18 µm thick layer of an Al braze clad alloy with 10 % silicon. The material was stretched by 6 % to simulate a sheet forming process prior to brazing. The deformation of 6 % was selected to optimize the occurrence of LFM, see Figure 2. A 60 x 20 mm^2 coupon was cut from the sample and placed in a furnace

with a nitrogen gas atmosphere. To simulate a brazing process the furnace was heated according to a heating ramp of 60 °C/min up to 500 °C, 25 °C/min between 500 and 575 °C and 15 °C/min between 575 and 590 °C. Immediately after reaching 590 °C, the heating process was interrupted. A temperature gradient over the sample was obtained through cooling blocks attached to both ends of the coupon. Hence, at the furnace temperature of 590 °C, the braze clad in the middle part of the coupon became liquefied while the braze clad at both ends remained solid. Between the non-"brazed" zone and the "brazed" zone there is a transition region. After the controlled atmosphere brazing (CAB) simulation the coupon was cut by electrical discharge machining (wire-cut type) into 1 mm wide and 40 mm long strips along the transition region from the non-"brazed" zone to the "brazed" zone at one half of the coupon, see Figure 4.

The analyzing method employed in the present study was the propagation-based imaging technique that uses the difference in refractive index for hard X-rays between particles and base material. The difference in refractive index will cause interference fringes as a consequence of the photon phase shift obtained when a coherent photon beam is illuminating different parts of the sample. Hence, the changes in the phase of the X-ray beam that passes through the sample will enhance the contrast of the X-ray absorption image. Images of the sample from different angles can then contribute to a 3D reconstruction through filtered back projection creating a phase-contrast X-ray computed tomography.

The phase-contrast X-ray computed tomography was performed at BL14-B2 beamline at the synchrotron radiation facility SPring-8 in Japan. The Al sample strip was illuminated by a monochromatic beam of 15 keV while the sample was rotated 180° with steps of 0.2°. The detector was a Hamamatsu Photonics C4880-41S combined with the imaging unit M11427-41. The image size was 4000 pixels x 2600 pixels and with an effective pixel size of 1.37 μm. The distance between the sample and the camera was 200 mm.

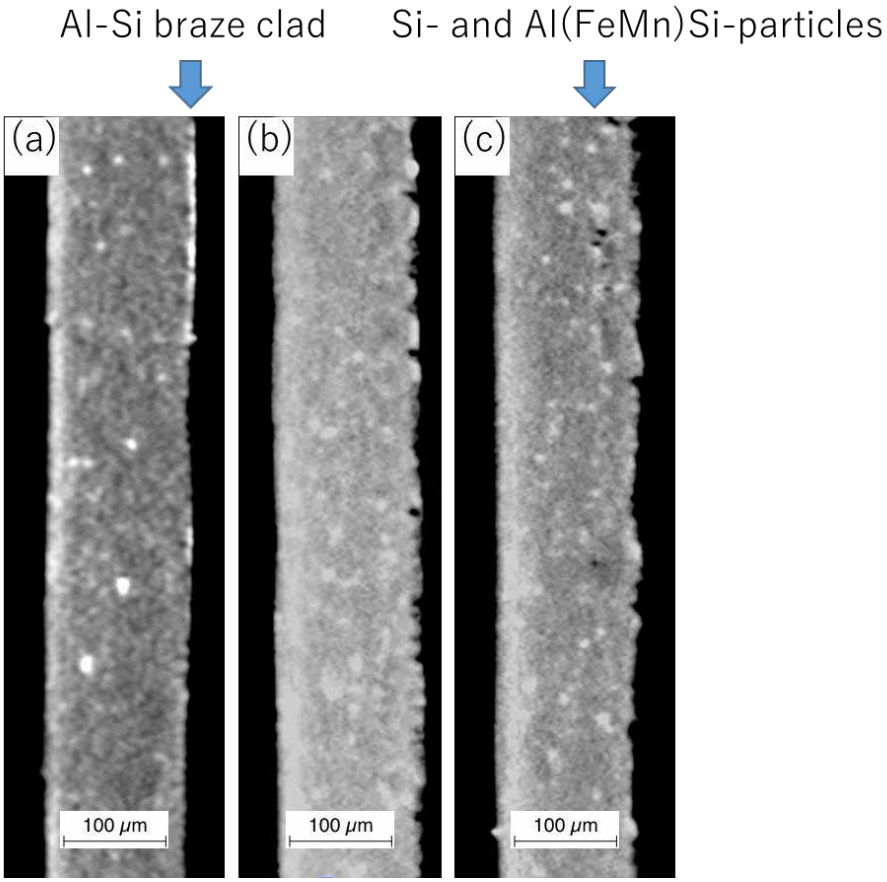

Fig. 5. Cross-section slices from the tomography imaging showing (a) the non-"brazed" zone, (b) the transition region between the non-"brazed" and the "brazed" zones, and (c) the fully "brazed" zone.

Results and Discussion

Three cross-sections of the Al-sample from the 3D image are presented in Figure 5 representing the non-"brazed" zone with an Al-Si braze clad on the right side of the cross-section, the transition region, and the fully "brazed" zone. PCX-CT is not able to distinguish different grains and the cross-section of the non-"brazed" zone in Figure 5(a) appears to be homogeneous with randomly distributed bright spots, which is precipitates of Al(FeMn)Si. The white bands of particles on the right side of the image are Si-particles that had segregated out from the Al-Si alloy braze clad. The transition region in Figure 5(b) is similar as the non-"brazed" zone as no grains are visible. It is, however, clear that the Al-Si alloy braze clad has molten, which gave the right side of the cross-section image a rough appearance. The 3DXRD showed that the grains in the braze clad with {001} orientation have grown larger at the elevated temperature [7]. In the fully "brazed" zone shown in Figure 5(c) the Al(FeMn)Si precipitates are randomly distributed in the left and middle part of the cross-section, similar as in Figure 5(a). On the right side, on the other hand, the precipitates are lining up at about 30 μm from the right end. The line-up formation of precipitates is highlighted with an arrow in Figure 5(c). Hence, when the Al-Si braze clad is molten in the fully "brazed" zone the PCX-CT shows an accumulation of relatively large precipitates decorating the borders of newly formed grains, which is characteristic features of LFM. For more information about grain formation in this particular sample see Ref. [7].

Figure 6 presents a cross-section image from a region that is between Figure (b) and (c), where the braze clad on the top of the Al sheet is molten. The captured image is selected because of the clear appearance of LFM on the left side where new particle-free Al-Si alloy grains are formed as a characteristic feature (highlighted with arrows). The absence of particles makes the new grains more grayish compared to the original grains in the core. The highlighted grains in Figure 6 show borders that appear white in the PCX-CT indicating that the new grains are decorated with a band of Si- and Al(FeMn)Si precipitates.

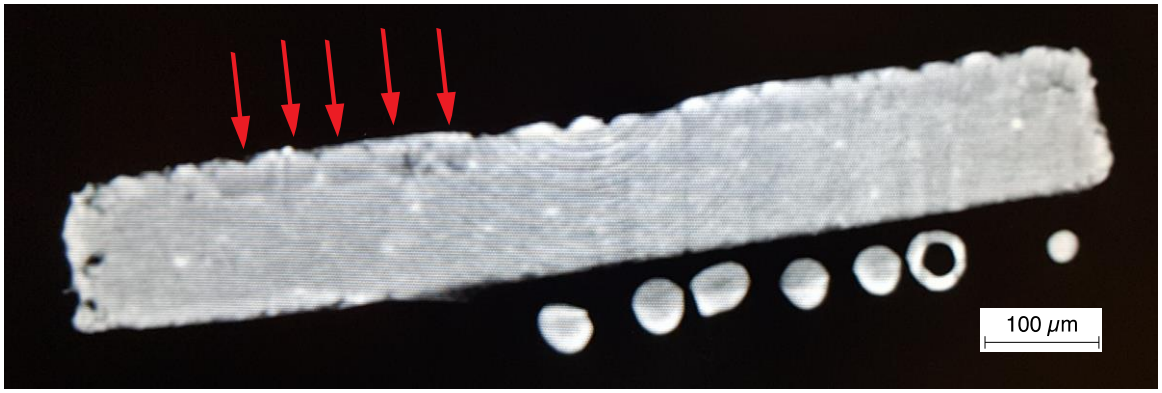

Fig. 6. A cross-section slice from the tomography imaging showing the molten braze clad on the top of the Al sample. Examples of new grains from LFM are highlighted with arrows. The balls under the Al sample are glass beads glued on the backside of the sample making it easier to identify the positions in the sample.

A closer look at one of the new grains formed after the LFM, the leftmost highlighted grain in Figure 6, is displayed in Figure 7(a). This new Al-Si alloy grain is free from particles, because the LFM has pushed all particles in front of the LFM frontline. Figure 7(b) shows an illustration of the new grains, colored gray, on top of the large grain in the core material (orange) [7]. The grain in the core material has randomly distributed Al(FeMn)Si-particles while the new Al-Si alloy grains are free from particles as they are pushed by the LFM frontline to the grain boundary.

The white band of Si- and Al(FeMn)Si-particles in the grain boundary of the new grains is sensitive toward corrosion attacks and may lead to inter-granular corrosion that severely weakens the material.

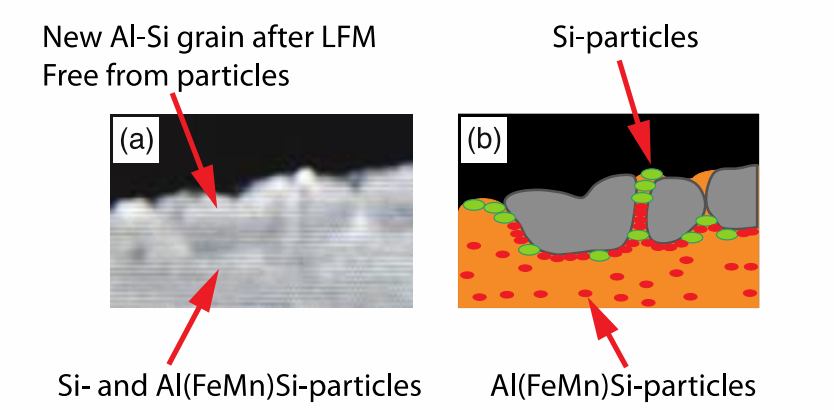

Fig. 7. (a) A new Al-Si alloy grain after LFM without particles. The new grain is decorated with Si- and Al(FeMn)Si-particles. (b) Illustration showing the new Al-Si alloy grain (gray) decorated with Si-particles (green) and Al(FeMn)Si-particles (red).

Figures 5-7 show that LFM in braze clad Al sheets can be identified in phase-contrast X-ray computed tomography after brazing. While the "brazed" zone showed severe occurrence of liquid film migration, the PCX-CT of the transition region between the non-"brazed" zone and the "brazed" zone shows that there are individual grains that could be distinguished by the particle accumulation around a particle-free surface grain, which is characteristic features of the LFM phenomenon. Hence, the result shows promises of new valuable information that can be extracted in combination with other 3D-imageing techniques, such as 3D-X-ray diffraction (3DXRD) and/or diffraction contrast tomography (DCT), as well as 2D-imaging techniques, such as light optical microscopy (LOM), scanning electron microscopy (SEM), and electron backscatter diffraction (EBSD).

Challenges

The performed study shows that it is possible to identify the transition region between the solid braze clad and the braze clad that was molten using phase-contrast X-ray computed tomography. Hence, it should be possible to find isolated grains formed after LFM in the tomography image. In addition, a closer investigation where the tomography image is merged with a 3D diffraction analysis might provide information regarding the close environment of the new grain formed after LFM. It should then be possible to reveal the grain orientation of the neighboring grains and if that has influences on the LFM phenomenon. Merging the two different images is, however, a delicate challenge.

Acknowledgements

We acknowledge SPring-8 for the provision of experimental facilities and the beam line scientist Kentaro Kajiwara at the Japan Synchrotron Radiation Research Institute. The research was partly funded by Sweden's Innovation Agency (Vinnova) through grants 2018-03268 and 2019-05299. The authors thank the metallurgical department at Gränges Finspång AB for microscopy work.

References

[1] M. Nylén *et al.*, *Materials Science Forum*, **217–222,** 1703 (1996).
[2] J. Lacaze *et al.*, *Mater. Sci. Eng. A*, **413-414**, 317 (2005).
[3] R. Woods, *Liquid film migration during aluminium brazing*, SAE International, 1997, 639.
[4] D. N. Yoon and W. J. Huppmann, *Acta Metallurgica*, **27**, 693 (1979).
[5] D. Y. Yoon, *Int. Mater. Rev.*, **40**, 149 (1995).
[6] M. J. Benoit *et al.*, *Metallurg. Mater. Transact. A*, **48**, 4645 (2017).
[7] T. Stenqvist *et al.*, *Adv. Eng. Mater.*, **23**, 2100126 (2021).
[8] Z. Hegedüs *et al.*, *IOP Conf. Ser.: Mater. Sci. Eng.*, **580**, 012032 (2019).
[9] D. McMorrow and J. Als-Nielsen, *Elements of Modern X-Ray Physics*, John Wiley & Sons, Inc., 2011, 318.
[10] S. C. Mayo *et al.*, *Opt. Express*, **11**, 2289 (2003).

[11] S. C. Mayo, A. W. Stevenson and S. W. Wilkins, *Materials*, **5**, 937 (2012).

(Received: September 21, 2022; Accepted: February 2, 2023; Published: April 28, 2023)